How to Test QE Neutrino-Nucleus Interaction Models using the Data of QE Lepton-Nuclear Interaction

Anatoli BUTKEVICH

Institute for Nuclear Research, Russian Academy of Science, 60th October Anniversary p.7A, Moscow 117312, Russia

Stanislav MIKHEYEV

Institute for Nuclear Research, Russian Academy of Science, 60th October Anniversary p.7A, Moscow 117312, Russia

Abstract

A widely used relativistic Fermi gas model and plane-wave impulse approximation approach are tested against electron-nucleus scattering data. Inclusive quasi-elastic cross section are calculated and compared with high-precision data for ^{12}C, ^{16}O, and ^{40}Ca. A dependence of agreement between calculated cross section and data on a momentum transfer is shown. Results for the ^{12}C(ν_μ, μ^-) reaction are presented and compared with experimental data of the LSND collaboration.

1. Introduction

A realistic description of neutrino-nucleus (νA) interactions at low- and intermediate-energy region is important for the interpretation of measurements by many neutrino experiments. The understanding of their sensitivity to neutrino properties, evaluation of the neutrino fluxes and spectra depend on the accuracy to which the νA cross sections are known. This is in particular crucial in analysis of the long-base line neutrino oscillation experiments in which the parameter of neutrino oscillation Δm^2 is determined using the total number of detected events and the distortions in the energy distribution of the detected muons caused by neutrino oscillation. On the other hand the neutrino-nucleus cross sections contain contributions from both axial-vector and vector currents and thus provide complementary information to that provided by electron-nucleus scattering, which is sensitive only to the nuclear vector current.

In many experiments the neutrino fluxes in sub-GeV and GeV energy region are used. At such energies the charged-current quasi-elastic (QE) neutrino-nucleus interactions give the main contribution to the detected events. Sizable nuclear effects have been observed in lepton scattering off nucleus at energies

less than a few GeV. They indicate that the nuclear environment plays an important role even at energies and momenta larger than those involved in typical nuclear ground state processes. The understanding of nuclear effects is relevant for the long-base line neutrino experiments in order to control the corresponding systematic uncertainties.

Many Monte-Carlo (MC) [1] codes developed for simulation of the neutrino detectors response are based on a simple picture of a nucleus as a system of quasi-free nucleons, *i.e.* relativistic Fermi gas model (RFGM) [2]. It takes into account Fermi motion of nucleons inside the nucleus and Pauli blocking effect. Unfortunately the lack of νA scattering data at low and intermediate energies doesn't allow to estimate the accuracy of this model. On the other hand, as follows from vast high-precision electron scattering data the RFGM neglects some important nuclear effects. So, the calculation of neutrino scattering off nucleus should first be tested against electron scattering data.

In the present work the electron QE cross sections are calculated in the framework of the RFGM and plane-wave impulse approximation (PWIA) [3,4,5] and compared with high-precision data for different nuclei. This comparison shows that the agreement between predictions of these models and data depends significantly on the momentum transfer to the target. We applied the RFGM and plane-wave impulse approximation to $^{12}C(\nu_\mu, \mu^-)$ reaction also.

The formalism of an inclusive charged current lepton-nucleus QE scattering is given in Sec.2. Results are presented and discussed in Sec.3 and some conclusions are drawn in Sec.4.

2. Formalism of the inclusive quasi-elastic scattering

In electromagnetic and weak charge current process electrons (neutrinos) interact with nuclei via the exchange of photons or W-boson and charged leptons are produced in the final state. In an inclusive reaction, in which incident electron (σ^{el}) or neutrino (σ^{cc}) with four-momentum $k_i = (\varepsilon_i, \mathbf{k}_i)$ is absorbed by nucleus with mass m_A and only the out-going lepton with four-momentum $k_f = (\varepsilon_f, \mathbf{k}_f)$ and mass m is detected, the cross section is given by contracting the lepton tensor and the nuclear tensor

$$d\sigma^{el} = \frac{\alpha^2}{Q^4} \frac{1}{|\mathbf{k}_i|\varepsilon_f} L_{\mu\nu}^{(el)} W^{\mu\nu(el)} d^3\mathbf{k}_f, \tag{1}$$

$$d\sigma^{cc} = \frac{G^2 \cos^2\theta_c}{2} \frac{1}{\varepsilon_i\varepsilon_f} L_{\mu\nu}^{(cc)} W^{\mu\nu(cc)} \frac{d^3\mathbf{k}_f}{(2\pi)^2}, \tag{2}$$

where $\alpha \simeq 1/137$ is the fine-structure constant, $G \simeq 1.16639 \times 10^{-11}$ MeV^{-2} is the Fermi constant, θ_c is the Cabbibo angle ($\cos\theta_c \approx 0.9749$), $Q^2 = -q^2 = (k_i - k_f)^2$,

and $q = (\omega, \mathbf{q})$ is the four-momentum transfer.

The lepton tensor can be written, by separating the symmetrical $l_S^{\mu\nu}$ and antisymmetric components $l_A^{\mu\nu}$ as

$$L^{\mu\nu(el)} = l_S^{\mu\nu}, \qquad L^{\mu\nu(cc)} = l_S^{\mu\nu} + l_A^{\mu\nu}, \qquad (3)$$

$$l_S^{\mu\nu} = 2(k_i^\mu k_f^\nu + k_f^\mu k_i^\nu - g^{\mu\nu} k_i \cdot k_f), \qquad (4)$$

$$l_A^{\mu\nu} = -2i\epsilon^{\mu\nu\alpha\beta} k_{i\alpha} k_{f\beta}, \qquad (5)$$

where $\epsilon^{\mu\nu\alpha\beta}$ is the antisymmetric tensor with $\epsilon^{0123} = -\epsilon_{0123} = 1$. The electromagnetic $W_{\mu\nu}^{(el)}$ and weak charged-current $W_{\mu\nu}^{(cc)}$ hadronic tensors are given by bilinear products of the transition matrix elements of the nuclear electromagnetic (weak charged current) operator $J_\mu^{(el)(cc)}$ between the initial nucleus state $|A\rangle$ of energy E_0 and final state $|B_f\rangle$ of energy E_f as

$$W_{\mu\nu}^{(el)(cc)} = \sum_f \int \langle B_f|J_\mu^{(el)(cc)}|A\rangle \times \langle A|J^{(el)(cc)\dagger}|B_f\rangle \delta(E_0 + \omega - E_f)dE_f, \qquad (6)$$

where the sum is taken over the undetected states.

The transition matrix elements are calculated in the first order perturbation theory and in impulse approximation, *i.e.* assuming that the incident lepton interacts with the single nucleon while other ones behave as spectators. The nuclear current operator $J_\mu^{(el)(cc)}(\mathbf{q})$ is taken as the sum of single-nucleon currents $j_\mu^{(el)(cc)}(\mathbf{q})$, *i.e.*

$$J_\mu^{(el)(cc)} = \sum_{i=1}^{A} j_i^{(el)(cc)},$$

with

$$j_\mu^{(el)} = F_V(Q^2)\gamma_\mu + \frac{i}{2M}F_M(Q^2)\sigma_{\mu\nu}q^\nu, \qquad (7)$$

$$j_\mu^{(cc)} = F_V(Q^2)\gamma_\mu + \frac{i}{2M}F_M(Q^2)\sigma_{\mu\nu}q^\nu + F_A(Q^2)\gamma_\mu\gamma^5 + F_P(Q^2)q_\mu\gamma^5, \qquad (8)$$

where M is the nucleon mass and $\sigma_{\mu\nu} = i[\gamma_\mu\gamma_\nu]/2$. F_V and F_M are the isovector Dirac and Pauli nucleon form factors, taken from Ref.[6]. F_A and F_P are axial and pseudo-scalar form factors, parametrized as

$$F_A(Q^2) = \frac{F_A(0)}{(1 + Q^2/M_A)^2}, \qquad F_P(Q^2) = \frac{2MF_A}{m_\pi^2 + Q^2}, \qquad (9)$$

where $F_A(0) = 1.267$, m_π is pion mass, and $M_A \simeq 1.032$ GeV is axial mass.

The general covariant form of the nuclear tensors is obtained in terms of two four-vectors, namely the four-momenta of target p^μ and q^μ. The electromagnetic and charged-current nuclear tensors can be written as

$$W^{\mu\nu(el)} = -W_1^{(el)}g^{\mu\nu} + \frac{W_2^{(el)}}{m_A^2}q^\mu q^\nu + \frac{W_3^{(el)}}{m_A^2}p^\mu p^\nu + \frac{W_4^{(el)}}{m_A^2}(p^\mu q^\nu + p^\nu q^\mu), \qquad (10)$$

$$W^{\mu\nu(cc)} = -W_1^{(cc)}g^{\mu\nu} + \frac{W_2^{(cc)}}{m_A^2}q^\mu q^\nu + \frac{W_3^{(cc)}}{m_A^2}p^\mu p^\nu + \frac{W_4^{(cc)}}{m_A^2}(p^\mu q^\nu + p^\nu q^\mu) +$$

$$+ \frac{W_5}{m_A^2}\epsilon^{\mu\nu\alpha\beta}q_\alpha p_\beta + \frac{W_6}{m_A^2}(p^\mu q^\nu - p^\nu q^\mu), \qquad (11)$$

where W_i are nuclear structure functions which depend on two scalars Q^2 and $p \cdot q$. Therefore, obtained from contraction between lepton Eqs.(3),(4),(5) and nuclear Eqs.(10),(11) tensors, the inclusive cross sections for the QE electron (neutrino)-nucleus scattering can be written as

$$\frac{d\sigma^{(el)}}{d\varepsilon_f d\Omega} = \sigma_M(v_L^{(el)}R_L^{(el)} + v_T^{(el)}R_T^{(el)}), \qquad (12)$$

$$\frac{d\sigma^{(cc)}}{d\varepsilon_f d\Omega} = \frac{G^2\cos^2\theta_C}{(2\pi)^2}k_f\varepsilon_f(v_0R_L^{(cc)} + v_TR_T^{(cc)} - v_{0L}R_{0L}^{(cc)} + v_{LL}R_{LL}^{(cc)} \pm v_{xy}^{(cc)}R_{xy}^{(cc)}), \qquad (13)$$

$$\sigma_M = \frac{\alpha^2\cos^2(\theta/2)}{4\varepsilon_i^2\sin^4(\theta/2)}, \qquad (14)$$

where σ_M is the Mott cross section and θ is the lepton scattering angle. The coefficients $v^{(el)}$ and v are obtained from lepton tensors components while the nuclear response functions $R^{(el)}$ and $R^{(cc)}$ are given in terms of components of nuclear tensors. The expressions for them can be found in Refs.[4],[7]. In order to evaluate nuclear response functions we consider the RFGM and PWIA approach based on assumption that the virtual photon interacts with off-shell nucleon and neglecting interaction of the knocked out nucleon with the residual nucleus. In the PWIA the four-momenta of the initial nucleus A, the bound off-shell nucleon N, and the final state B are

$$p \equiv (m_A, \mathbf{0}), \qquad p \equiv (m_A - (\mathbf{p}^2 + m_B^{*2})^{1/2}, \mathbf{p}), \qquad p_B \equiv ((\mathbf{p}^2 + m_B^{*2})^{1/2}, -\mathbf{p}),$$

respectively. Here $m_B^* = m_B + \varepsilon_f$, m_B^* and ε_f are the mass and intrinsic energy of the final (A-1)-nucleon state, respectively. Within the above assumption the nuclear structure functions can be written in as follows

$$W_i^{A(el)} = \int d\mathbf{p} \int dE Z S^p(|\mathbf{p}|, E) \sum_{j=1}^{2} C_{ij} W_j^{p,off}(Q^2) \qquad (15)$$
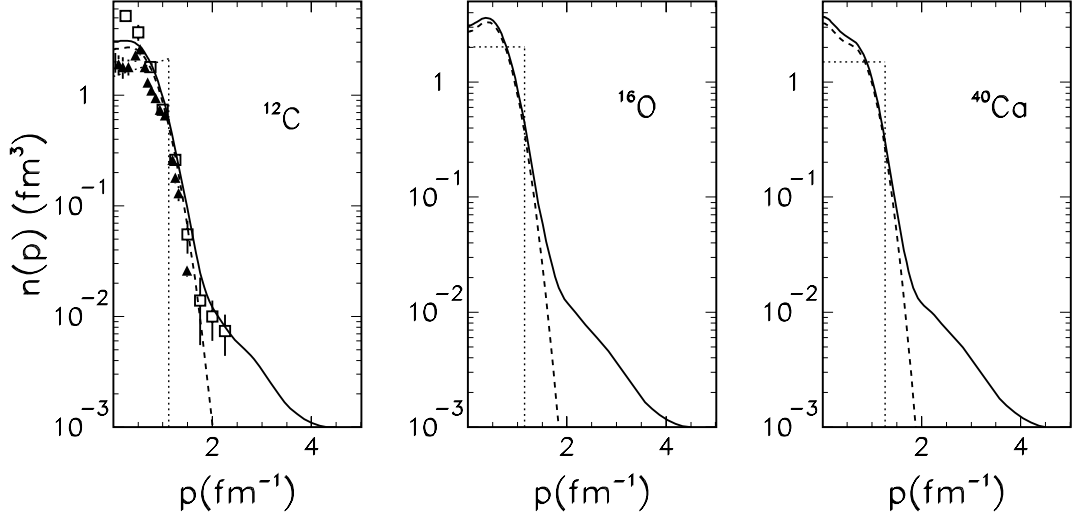
Fig 1. Nucleon momentum distribution corresponding to Eq.(28) (solid lines) and Eq.(26) (dotted lines). The momentum distribution n_0 is given by dashed line. The open squares represent results obtained in Ref.[8]. The full triangles represent the values of $n_0(p)$ obtained in Ref.[9].

$$+ \text{ (similar terms for the neutrons),}$$

$$W_i^{A(cc)} = \int d\mathbf{p} \int dE (A-Z) S^n(|\mathbf{p}|, E) \sum_{j=1}^{5} D_{ij} W_j^{n,off}(Q^2). \qquad (16)$$

Here, Z is the number of protons, $W_j^{N,off}(N = p,n)$ are the off-shall nucleon structure functions that are given in the terms of nucleon form-factors. C_{ij} and D_{ij} are kinematic factors whose explicit form depends on the treatment of off-shell effects, and $S^N(|\mathbf{p}|, E)$ is the nucleon spectral function. In this paper we assume that $W_j^{N,off}$ are identical to free nucleon structure function W_j^N. The parametrization of W_j^N is taken from Refs.[2,3]. The nucleon spectral function $S^N(|\mathbf{p}|, E)$ in the PWIA represents probability to find the nucleon with the momentum $\mathbf{p}$ and the removal energy E in the ground state of the nucleus. In the commonly used Fermi gas model, that was described by Smith and Moniz [2], nucleons in nuclei are assumed to occupy plane wave states in uniform potential while the knocked-out nucleon is outside of the Fermi sea. The Fermi gas model provides the simplest form of the spectral function which is given by

$$S_{FG}(E, |\mathbf{p}|) = \frac{3}{4\pi p_F^3} \Theta(p_F - |\mathbf{p}|) \Theta(|\mathbf{p} + \mathbf{q}| - p_F) \delta[(|\mathbf{p}|^2 + M^2)^{1/2} - \epsilon_b - E)], \quad (17)$$

where p_F denotes the Fermi momentum and a parameter ϵ_b is effective bind-
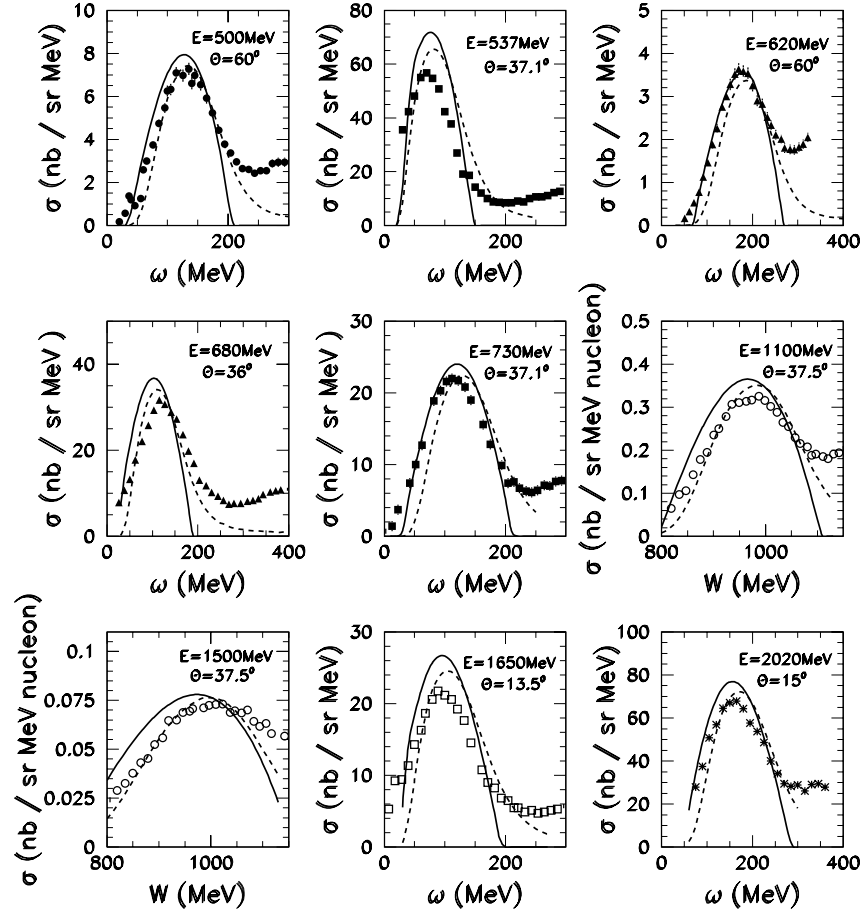
Fig 2. Comparison of theoretical and experimental cross sections for ^{12}C. The data are taken from Refs.[10] (filled circles), [11] (filled squares), [12] (filled triangles), [13] (open circles), [14] (open squares), and [15] (stars).

ing energy, introduced to account of nuclear binding. The QE lepton-nucleus reactions are complicated processes, involving nuclear many body effects. The calculation of the nuclear spectral function for complex nuclei requires to solve many body problem. In this paper we consider also a phenomenological model using PWIA approach with the spectral function which incorporates both the single particle nature of the nucleon spectrum at low energy and high-energy and high momentum components due to NN-correlations in ground state. Following [4,5] we separate the full spectral function into two parts

$$S(E, \mathbf{p}) = S_0(E, \mathbf{p}) + S_1(E, \mathbf{p}). \tag{18}$$

The integration of Eq.(18) over energy gives nucleon momentum distribution,

$$n(\mathbf{p}) = \int \frac{dE}{2\pi} S(E, \mathbf{p}) = n_0(\mathbf{p}) + n_1(\mathbf{p}). \tag{19}$$
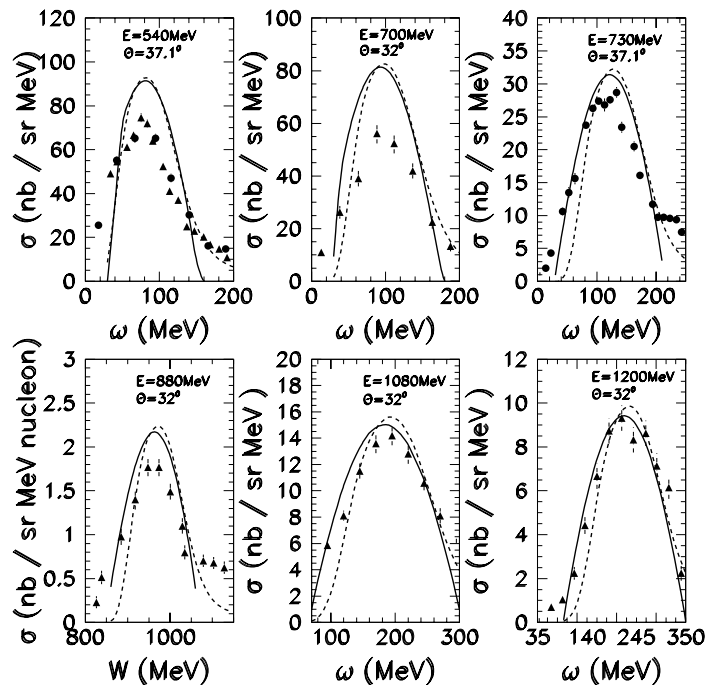
Fig 3. Comparison of theoretical and experimental cross sections for ^{16}O. The data are taken from Refs.[11] (filled circles), and [16] (filled triangles).

The spectral function is normalized according to

$$\int \frac{dEd\mathbf{p}}{2\pi} S(E, \mathbf{p}) = 1. \tag{20}$$

The detailed description of this model is given in Refs.[4,5] as well as parametrization of $n_0(\mathbf{p})$ and $n_1(\mathbf{p})$, which fit the result of many-body calculations of nuclear momentum distribution. As follows from these calculations the low momentum part incorporates about 80% of the total normalization of spectral function, while the other 20% are taken by the high momentum part. The nucleon momentum distributions $n(|\mathbf{p}|)$ and $n_{FG}(|\mathbf{p}|)$ are shown in Fig.1. The normalization of $n(p)$ and $n_{FG}(p)$ is $\int dpp^2 n(p) = 1$, where $p = |\mathbf{p}|$. The distributions n_{FG} for various nucleus ^{12}C, ^{16}O and ^{40}Ca were calculated using the value of parameters $p_F = 221$ MeV, $\epsilon_b = 25$MeV (^{12}C), $p_F = 225$ MeV, $\epsilon_b = 27$ MeV (^{16}O), and $p_F = 249$ MeV, $\epsilon_b = 33$MeV) (^{40}Ca) [10].

3. Results

There is vast high-precision data for electron scattering off nucleus ^{12}C, ^{16}O, and ^{40} Ca. Hence these nuclei are taken at the focus of the present work. Data on inclusive cross sections for a number of nuclei (A between 6 and 208)
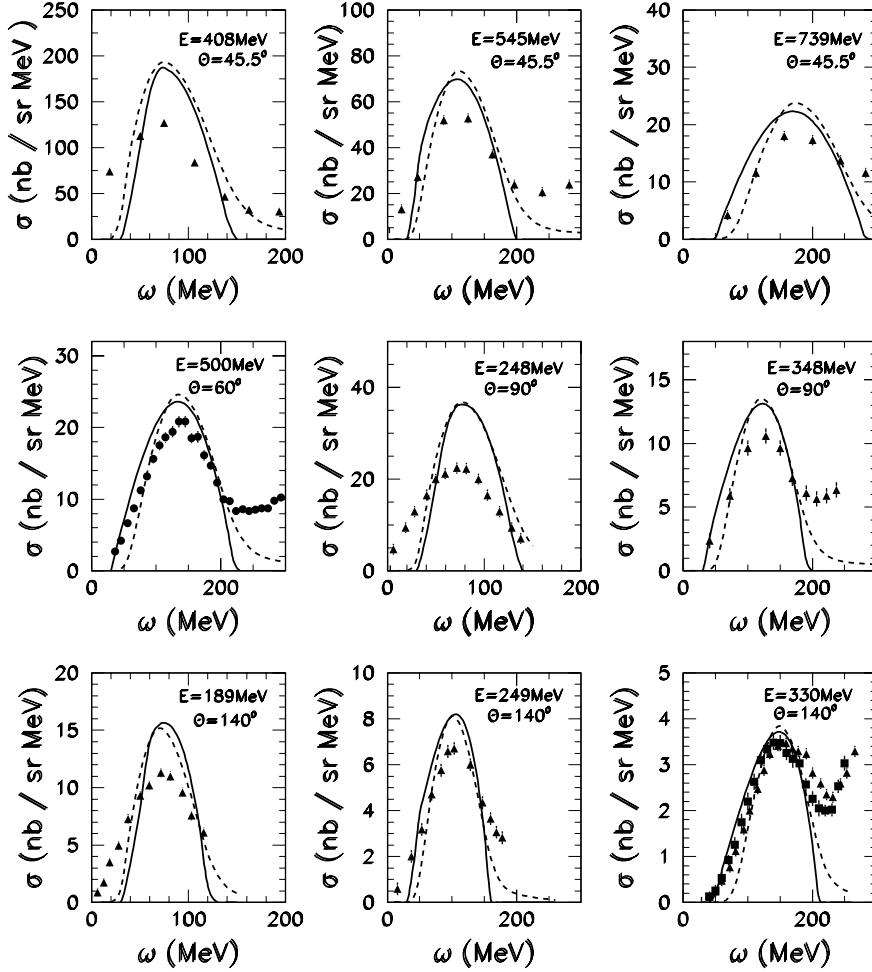
Fig 4. Comparison of theoretical and experimental cross sections for ^{40}Ca. The data are taken from Refs.[10] (filled circles), [17] (filled squares), and [18] (filled triangles).

with same kinematics were obtained early in Ref.[10]. Carbon data are available from experiments [11]-[15]. For oxygen target the experiments were performed by SLAC [11] and Frascaty [16] groups. For calcium target the inclusive cross section have been measured in experiments [10], [17]-[19]. All these data were used in our analysis.

Using both the relativistic Fermi gas model and the PWIA approach described above, we calculated the inclusive cross sections for given kinematics (energies and angles) and compared them with data. The results are presented in Figs.2,3,4 for ^{12}C, ^{16}O, and ^{40}Ca respectively. The solid lines are the results in the Fermi gas model, while short-dashed lines are results in the PWIA. The differences can be seen from these figures in which the cross sections as functions
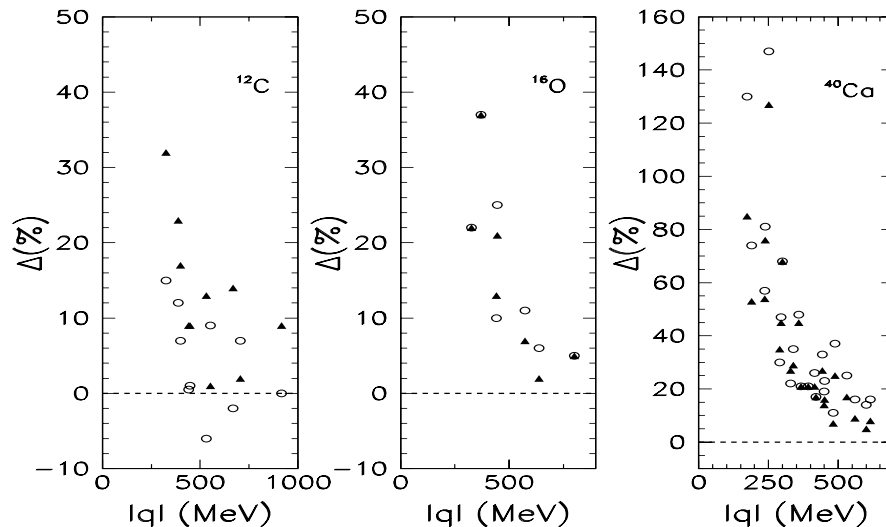
Fig 5. Differences between calculated and measured values of cross sections at maximum for ^{12}C, ^{16}O, and ^{40}Ca as functions of three-momentum transfer $|\mathbf{q}|$. The filled triangles correspond to the Fermi gas model results and open circles correspond to the PWIA approach.

of ω or invariant mass produced on a free nucleon W are plotted. At the maximum of the cross sections both models overestimate the measured values. We evaluated the differences between predicted (σ_{cal}) and measured (σ_{data}) quantities $\Delta = \sigma_{calc} - \sigma_{data}$. $\Delta(|\mathbf{q}|)$ as a function of three-momentum transfer $|\mathbf{q}|$, is shown in Fig.5, from which it is clear that the $\Delta(|\mathbf{q}|)$ decreases with $|\mathbf{q}|$ from 30÷50% at $|\mathbf{q}| \leq 200$ MeV to 10÷15% at $|\mathbf{q}| \geq 500$ MeV.

In Refs.[17], [18] transverse $R_T^{(el)}$ and longitudinal $R_L^{(el)}$ response functions have been extracted for 200 MeV$\leq |\mathbf{q}| \leq 500$ MeV. It has been shown that the relativistic Fermi gas model overestimates the observed longitudinal response for about 40% [17] ($\sim$20% [18]). At low $|\mathbf{q}|$ this model also overestimates the magnitude of the transverse response function. At high $|\mathbf{q}|$ the model reproduces $R_T^{(el)}$ better.

The predictions of both models are compared with the experimental result of the LSND collaboration at Los Alamos for ^{12}C(ν_μ, μ^-) reaction [20]. The calculations are flux-averaged over the Los Alamos neutrino flux. The mean energy of neutrino flux above threshold is 156 MeV. The comparison is shown in Fig.6 where the calculated muon energy distributions are normalized to the experimental total number events. We note that both models do not give an accurate descriptions of the shape of the muon spectrum. The flux-averaged cross section integrated over the muon energy is 17.8×10^{-40} cm^2 in the case of the RFGM and 26.8×10^{-40} cm^2 in the PWIA. The experimental value is (10.6±0.3±1.8)×10^{-40} cm^2. The result

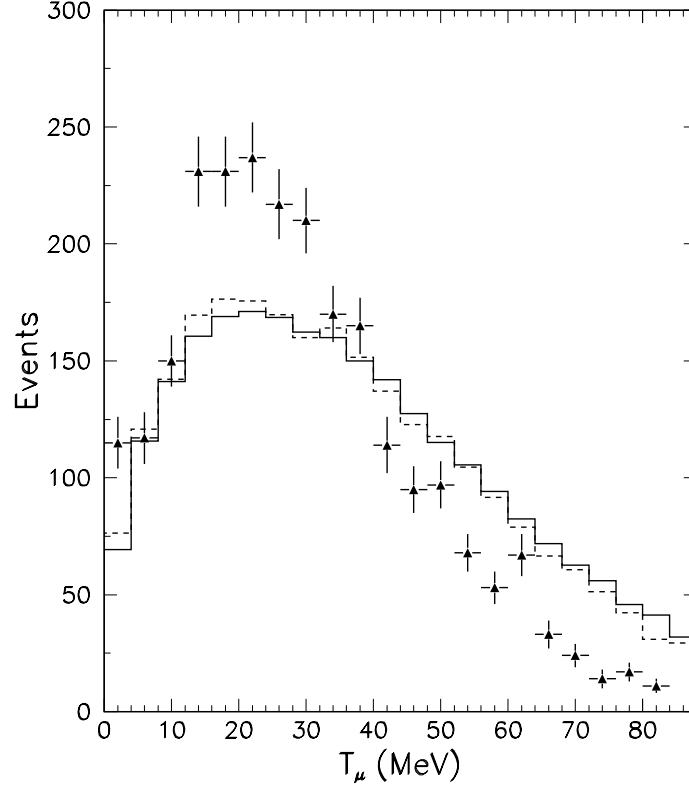**Fig 6.** The distribution of muon kinetic energy for inclusive ^{12}C (ν_μ, μ^-) reaction. Experimental data from Ref.[20]. The results of the RFGM (solid linen histogram) and the PWIA approach (short-dashed line histogram) are normalized to the data.

obtained by other calculation in the framework of the Fermi gas model with local density approximation [21] gives also larger value $\sigma=(16.7 \pm 1.37)\times 10^{-40}$ cm^2.

4. Conclusions

In this work we have tested the widely used relativistic Fermi gas model and plane-wave impulse approximation approach against electron-nucleus scattering data. We calculated the inclusive QE cross sections and compared them with high-precision data for ^{12}C, ^{16}O, and ^{40}Ca in a wide region of incident energy and momentum. We evaluated the differences Δ between predicted and measured QE cross section at the maximum and found that both models overestimate the measured values. The function $\Delta(|\mathbf{q}|)$ decreases with three-momentum transfer from 30÷50 % at $|\mathbf{q}| \leq 200$ MeV to 10÷15 % at $|\mathbf{q}| \geq 500$ MeV. Therefore these models overestimate also the cross sections at low $Q^2 = |\mathbf{q}|^2 - \omega^2$.

We applied the RFGM and PWIA approach to ^{12}C(ν_μ, μ^-) reaction. The flux-averaged total cross sections and muon energy distributions were calculated

and compared with experimental results of the LSND collaboration. The calculated cross sections are significantly larger than the experimental ones and both models do not give an accurate description of the shape of muon spectrum.

In conclusion we note that the inclusion of final state interaction effects along with realistic spectral function may significantly correct the description of the data at low momentum transfer, as was pointed in Refs.[7],[16].

5. Acknowledgments

References

[1] G. P. Zeller, arXiv:hep-ex/0312061.
[2] R. A. Smith, and E. J. Moniz, Nucl. Phys. B101 (1975) 547.
[3] J. J. Kelly, Adv. Nucl. Phys. 23 (1996) 75.
[4] C. Ciofi degli Atti, and S. Simula, Phys. Rev. C53 (1996) 1689.
[5] S. A. Kulagin, and R. Petti, arXiv:hep-ph/0412425.
[6] M. J. Musolf, and T. W. Donnelly, Nucl. Phys. A546 (1992) 509.
[7] A. Meucci, C. Giusti, and D. Pacati, Nucl. Phys. A739 (2004) 277.
[8] C. Ciofi degli Atti, E. Pace, and G. Salme, Phys. Rev. C43 (1991) 1153.
[9] S. Frullani, and J. Mougey, Adv. Nucl. Phys. 14 (1981) 1.
[10] R. Whitney et al., Phys. Rev. C9 (1974) 2230.
[11] J. S. O'Connell et al., Phys. Rev. C35 (1987) 1063.
[12] P. Barreau et al., Nucl. Phys. A402 (1983) 515.
[13] R. M. Sealock et al., Phys. Rev. Lett. 62 (1989) 1350.
[14] D. Baran et al., Phys. Rev. Lett. 61 (1988) 400.
[15] D. Day et al., Phys. Rev. C48 (1993) 1819.
[16] M. Anghinolfi et al., Nucl. Phys. A602 (1996) 402.
[17] M. Deady et al., Phys. Rev. C33 (1986) 1987.
[18] C. Williamson et al., Phys. Rev. C56 (1997) 3152.
[19] Z. Meziani et al., Phys. Rev. Lett. 54 (1985) 1233.
[20] L. B. Auerbach et al., Phys. Rev. C66 (2002) 015501.
[21] S. K. Singh, N. C. Mukhopadhyay, and E. Oset, Phys. Rev. C57 (1998) 2687.